SEETE
Scientific Experiences in Energy and Thermal Engineering
Shaping the Future of Sustainable Energy and Thermal Engineering
AISINDONESIA
ACADEMICIAN • INDUSTRY• SOCIETY
ISSN: 3164-8533
https://doi.org/10.68252/seete.17
Vol. 1, No. 1 (2027), pp. e17.1-12
Research Article

Kinetic Analysis of the Combustion Reaction of Sub-Bituminous Coal Blended with Empty Fruit Bunch (EFB) Waste

Akhmad Faruq Alhikami[1,2], Nurcholis Majid[1], Ena Marlina[1,2*], Ria Aniza[3]

[1]Universitas Islam Malang, Malang, Indonesia
[2]Agro-Renew Centre for energy, Water, and Environment Technologies, Universitas Islam Malang, Indonesia
[3]Université de Lorraine, INRAE, LERMAB, F88000, Epinal, France

*Corresponding author: ena.marlina@unisma.ac.id

Copyright © The Author(s). This work is licensed under a Creative Commons Attribution-NonCommercial 4.0 International License. Published by AIS Indonesia

Article History: Received: 11 September 2026 | Revised: 13 October 2026 | Accepted: 15 October 2026 | Published online: 18 October 2026

Abstract

This study evaluated the effect of blending ratios of sub-bituminous coal and Empty Fruit Bunch (EFB) biomass on the activation energy (E_a) of the combustion process using Thermogravimetric Analysis (TGA) and the Coats–Redfern kinetic approach. The fuel samples consisted of 100% coal, 80% coal–20% EFB, and 60% coal–40% EFB blends. The results showed that the average activation energy during Stage I decreased from 91.16 kJ/mol for pure coal to 86.69 kJ/mol for the 20% EFB blend, before increasing to 91.64 kJ/mol for the 40% EFB blend. During Stage II, the activation energy decreased from 61.88 kJ/mol for pure coal to 48.70 kJ/mol for the 20% EFB blend, and then increased slightly to 49.50 kJ/mol for the 40% EFB blend. These findings indicate that the addition of 20% EFB produces a synergistic effect by enhancing the thermal reactivity of the fuel mixture, whereas increasing the EFB content to 40% results in a higher activation energy due to the greater complexity of lignin decomposition and the formation of an ash layer on the char surface. It can therefore be concluded that the 20% EFB blend represents the optimum co-firing ratio from a kinetic perspective.

Keywords: Activation energy; Co-firing; Sub-bituminous coal; Empty Fruit Bunch (EFB); Thermogravimetric Analysis (TGA); Coats–Redfern method; Combustion kinetics

1. Introduction

Coal remains the backbone of electricity supply in Indonesia. In 2023, coal-fired power plants accounted for approximately 55% of the national installed generation capacity of 91.1 GW, and the average emission intensity of the electricity sector reached 0.919 t CO_2 /MWh [1]. This strong dependence on coal makes the power sector a major source of greenhouse gas (GHG) emissions and a key challenge for Indonesia's Enhanced Nationally Determined Contribution, which targets an unconditional GHG emission reduction of 31.89% relative to the business-as-usual level by 2030 [1]. Reducing the carbon intensity of the existing coal-fired power plants is therefore an urgent component of the national energy transition.

Biomass co-firing, i.e., the partial substitution of coal with biomass in existing coal-fired boilers, is widely regarded as one of the most practical near-term decarbonization options because it requires relatively limited modification of the existing infrastructure and can reduce net CO_2, SO_x, and NO_x emissions [2]. In Indonesia, co-firing trials were initiated by the state electricity company in 2019, and by 2023 the program had been implemented in more than 40 coal-fired units at biomass blending ratios of 1–5% [[1]. Pilot tests in pulverized-coal boilers at 5% co-firing showed that the plant efficiency changes in accordance with the heating value of the biomass and that SO_2 and NO_x emissions can be reduced [3], while techno-economic assessments have begun to evaluate higher co-firing ratios in combination with carbon capture and storage [4].

Among the available biomass resources, palm oil industry residues represent the largest share of Indonesia's technical biomass potential, at approximately 170.5 PJ per year [1], and oil palm residues such as empty fruit bunches (EFB), shells, and fibres have been identified as major contributors to the national bioenergy potential [5]. The processing of one tonne of fresh fruit bunches generates approximately 23% EFB, 6.5% shells, and 13% fibre [6]. EFB has a low commercial value, and the large quantities continuously generated by palm oil mills create disposal problems [7], although simulation studies have shown that oil palm solid wastes, including EFB, can be utilized for electricity generation [8].

However, the fuel properties of EFB differ considerably from those of coal. EFB has a lignocellulosic structure with a high volatile matter content, and its ash contains potassium, calcium, and silicon, which may cause fouling,

slagging, and ash melting during combustion [7], [9]. Pilot-scale investigations in Indonesia showed that co-firing coal with 25% EFB–frond mixtures provided good combustion performance but increased the slagging tendency, as indicated by reduced ash fusion temperatures and the formation of sticky deposits [10], and combined theoretical and experimental ash investigations have been used to assess the suitability of several biomasses, including EFB–frond mixtures, as co-firing fuels for pulverized-coal boilers [11]. Slagging and fouling caused by the alkali and silica contents of co-fired fuels have also been reported for refuse-derived fuel [12] and biochar [13]. Consequently, the biomass blending ratio must be selected to balance combustion reactivity against ash-related operational risks.

Thermogravimetric analysis (TGA) is widely used to characterize the thermal behavior and kinetics of solid fuels and their blends. For oil palm biomass, TGA-based studies have quantified the pyrolysis and combustion kinetics of various residues [14], [15] and the influence of torrefaction on combustion kinetics [16]. For coal–oil palm biomass blends, the addition of biomass improved the ignition and burnout characteristics of sub-bituminous coal and reduced the apparent activation energy [17], whereas coal–EFB blends analyzed under an inert atmosphere exhibited non-additive behavior, indicating interactions between the two fuels [18]. More recently, combustion and thermodynamic indices were used to identify an optimal coal–oil palm biomass blend [19]. Studies on other coal–biomass systems have shown that blending can enhance the maximum mass-loss rate and lower the ignition and burnout temperatures, with 20% biomass identified as the optimum ratio based on combustion indices [20], and that the minimum activation energy may occur at an intermediate rather than the highest biomass ratio [21]. Such interactions have been attributed to both the catalytic effect of minerals in biomass ash and the non-catalytic effect of biomass volatiles [22], and the extent of these synergistic effects depends on the blending ratio [23] and on the lignocellulosic components involved [24].

Kinetic analysis provides parameters such as the activation energy (Ea), the pre-exponential factor (A), and the most probable reaction mechanism, which are essential for modeling and optimizing co-firing processes. The integral Coats–Redfern method is a model-fitting approach that estimates these parameters from TGA data obtained at a single heating rate by testing a set of solid-state reaction functions $g(\alpha)$ [25], [26][. Kinetic mechanisms have been evaluated for coal–biomass blends during co-pyrolysis [27] and co-combustion [21], and the Coats–Redfern method has been applied to oil palm solid wastes [28] and to EFB, whose decomposition subdivisions were best described by different reaction models [29]. The pyrolysis behavior of EFB-derived hydrochars has also been examined [30]. Nevertheless, the ICTAC Kinetics Committee recommendations emphasize that kinetic parameters obtained by model fitting should be interpreted with caution, particularly when a single heating rate is used [31].

Despite these studies, the stage-wise combustion kinetics of sub-bituminous coal blended with EFB under an oxidative atmosphere, evaluated across a broad set of reaction models, have received limited attention, and the effect of increasing the EFB fraction from 20% to 40% on the dominant reaction mechanism and the activation energy remains unclear. Therefore, this study investigated the combustion of 100% sub-bituminous coal and its blends containing 20% and 40% EFB using TGA in air. The objectives were (i) to characterize the mass degradation profiles of the fuels, (ii) to identify the dominant decomposition kinetic model in each combustion stage using eleven Coats–Redfern reaction models, and (iii) to determine the activation energy of each fuel in order to identify the most favorable blending ratio from a kinetic perspective. The study was limited to laboratory-scale TGA data; the combustion performance in a boiler, flue gas emissions, and ash characteristics were not evaluated.

2. Methods

This study employed an experimental method based on a theoretical approach, with data processing conducted through an experimental simulation approach. The tests were carried out directly on the combustion process of sub-bituminous coal blended with Empty Fruit Bunches (EFB) in a co-firing system using the Coats-Redfern method. Sample preparation was carried out at the Integrated Laboratory of Universitas Islam Malang, Malang, East Java, Indonesia, whereas the thermogravimetric analysis (TGA) was performed at the Integrated Laboratory of the Faculty of Agricultural Technology, Universitas Brawijaya, Malang, East Java, Indonesia. The study was conducted from October 2024 to January 2025.

2.1. Variables

The independent variable of this study was the fuel composition, namely 100% sub-bituminous coal (100% COAL), a blend of 80% coal and 20% EFB (EFB 20%), and a blend of 60% coal and 40% EFB (EFB 40%) on a mass basis. The dependent variables were the combustion characteristics derived from the TGA data, namely the mass degradation profile, the dominant decomposition kinetic model, and the kinetic parameters (activation energy and pre-exponential factor) obtained using the Coats–Redfern method. The controlled variables were the TGA operating conditions, namely a heating rate of 10 °C/min, a maximum temperature of 1000 °C, and an air flow rate of 60 mL/min, together with the particle size and the sample mass prepared for each fuel.

2.2. Equipment and Materials

The raw materials used in this study were sub-bituminous coal and oil palm EFB. The samples were prepared using a blender to crush the raw materials, a 200-mesh sieve to obtain a uniform particle size, aluminum foil and trays to hold the material during sieving, and an analytical balance to weigh the fuel components. The thermal decomposition tests were performed using a thermogravimetric analyzer. The experimental data were processed using Microsoft Excel, whereas the TGA–DTG curves, the kinetic plots, and the linear regressions were produced using Origin software.

2.3. Procedure

The EFB was dried, ground, and sieved until a uniform particle size was obtained. The sub-bituminous coal was crushed, ground, and sieved to the same particle size as the EFB. The grinding and sieving steps were repeated until sufficient fine powder was available for the thermogravimetric tests.

The prepared coal and EFB powders were then blended at coal-to-EFB mass ratios of 80:20 and 60:40, while pure coal was used as the reference fuel. The components were mixed manually until a homogeneous mixture was obtained, because homogeneity is essential to ensure the reproducibility and consistency of the combustion tests. For each fuel, 1 g of sample was weighed using a high-precision analytical balance to ensure a consistent amount of material in every test.

2.4. Fuel Testing

Prior to the experiment, the fuel samples were prepared according to the predetermined blending ratios, followed by the preparation and calibration of the Thermogravimetric Analysis (TGA) instrument and other supporting equipment to ensure accurate measurements. The TGA test was conducted under controlled operating conditions with a heating rate of 10°C/min, a maximum temperature of 1000°C, and air as the carrier gas at a constant flow rate of 60 mL/min. During the combustion process, the TGA system continuously recorded the changes in sample mass as a function of temperature and time, allowing the thermal decomposition behavior of the fuel blends to be monitored throughout the experiment. Upon completion of the test, the instrument was allowed to cool to room temperature before cleaning was performed to prepare it for subsequent experiments. Finally, the experimental data obtained from the TGA measurements were processed and analyzed to evaluate the thermal degradation characteristics and combustion kinetics of the coal–biomass blends using the analytical procedures described in the following section.

2.5. Data Analysis

The rate of mass loss (DTG) was obtained as the first derivative of the TGA curve with respect to time, as expressed in Eq. (1), and the TGA and DTG curves of each sample were plotted together in a single graph.

$$DTG = \frac{dm}{dt} \tag{1}$$

The kinetic parameters were determined using the integral Coats–Redfern method [25], [26]. The degree of conversion (α) was calculated from the TGA data using Eq. (2), where m_0 is the initial sample mass, m_t is the sample mass at time t, and m_f is the final sample mass of the corresponding stage.

$$\alpha = \frac{m_0 - m_t}{m_0 - m_f} \tag{2}$$

The Coats–Redfern equation is expressed in Eq. (3). Because $2RT/E_a \ll 1$, this term can be neglected, yielding the linear form given in Eq. (4).

$$\ln\left[\frac{g(\alpha)}{T^2}\right] = \ln\left[\frac{AR}{\beta E_a}\left(1-\frac{2RT}{E_a}\right)\right] - \frac{E_a}{RT} \tag{3}$$

$$\ln\left[\frac{g(\alpha)}{T^2}\right] = \ln\left[\frac{AR}{\beta E_a}\right] - \frac{E_a}{RT} \tag{4}$$

In these equations, g(α) is the integral form of the reaction mechanism function, T is the absolute temperature (K), β is the heating rate (10 K/min), A is the pre-exponential factor (min^{-1}), E_a is the activation energy (kJ/mol), and R is the universal gas constant (8.314×10^{-3} kJ/mol·K). For each combustion stage, $\ln[g(\alpha)/T^2]$ was plotted against 1/T for eleven solid-state reaction models, namely the reaction-order (F1–F3), diffusion (D1–D4), Avrami–Erofeev nucleation (A2–A3), and geometrical contraction (R2–R3) models [25], [32]. The slope of each regression line is equal to $-E_a/R$ and the intercept is equal to $\ln[AR/(\beta E_a)]$; therefore, E_a and A were calculated using Eqs. (5) and (6). The absolute values of the slopes are reported in Table 2.

$$E_a = -\text{slope} \times R \tag{5}$$

$$A = \frac{\beta E_a}{R}\exp(\text{intercept}) \tag{6}$$

The model with the highest coefficient of determination (R^2) was regarded as the dominant reaction mechanism for each stage, whereas the average E_a over all eleven models was used to compare the fuel blends. The regression analysis was performed using Origin software, and the experimental data were processed using Microsoft Excel.

3. Results and Discussion

3.1. Research Data

Based on the results obtained during the data collection process, the findings are presented according to the research activities that were carried out. This study was conducted at the Integrated Laboratory of Universitas Islam Malang using basic laboratory equipment. The initial stage involved crushing sub-bituminous coal and Empty Fruit Bunch (EFB) biomass samples using a blender until they were converted into powder. The powder was then sieved using a 200-mesh sieve to obtain the required particle size. Subsequently, sub-bituminous coal and EFB biomass were blended at three different mixing ratios: 100% coal, 80% coal/20% EFB, and 60% coal/40% EFB, using an analytical balance with a total sample mass of 1 g. The grinding and sieving processes were repeated several times to ensure the availability of sufficient fine powder for Thermogravimetric Analysis (TGA).

The TGA tests were then conducted on the co-firing samples with blending ratios of 100% coal, 80% coal/20% EFB, and 60% coal/40% EFB, using a maximum temperature of 1000°C, a heating rate of 10°C/min, and air as the reactive atmosphere at a flow rate of 60 mL/min. The analysis included the determination of combustion reaction kinetics, such as the mass degradation rate, decomposition kinetic model, and activation energy. The TGA data were further analyzed using the Coats-Redfern method to obtain the reaction kinetic parameters.

3.2. Mass Degradation Profile

Thermogravimetric Analysis (TGA) and Derivative Thermogravimetry (DTG) are effective methods for evaluating the combustion characteristics of solid fuels by monitoring changes in mass as a function of temperature. The TGA curve illustrates the reduction in sample mass during the heating process, whereas the DTG curve provides information on the rate of mass loss at specific temperatures. Table 1 presents the weight loss data and temperature ranges corresponding to the two stages of thermal degradation for three different fuel compositions,

Table 1. Mass degradation profile

Material	Weight loss %	Range temperature/ Weight loss			
		Stage I (°C)	Weight loss (%)	Stage II (°C)	Weight loss (%)
COAL 100%	95.427%	27.81 – 128.78	8.007	240.21 – 968.21	80.30
EFB 20%	99.08%	27.3 – 148.3	13.767	185.5 – 966.3	82.23
EFB 40%	92.196%	27.63 – 144.1	9.1200	185.2 – 965.75	81.45

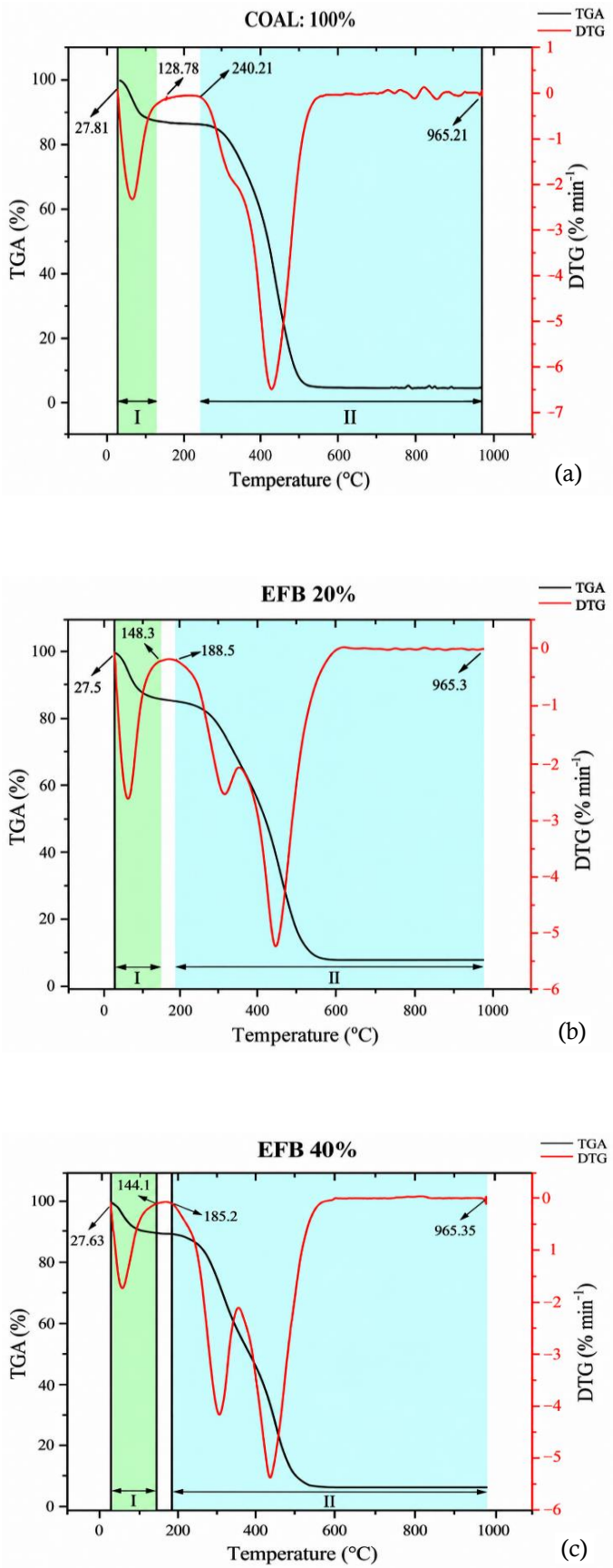


Figure 1. Mass degradation profile curves: (a) Coal 100%, (b) EFB 20%, and (c) EFB 40%

namely pure sub-bituminous coal (100% COAL), a coal blend containing 20% Empty Fruit Bunch (EFB), and a coal blend containing 40% EFB. **Figure 1** shows the corresponding TGA-DTG curves for each sample.

For the 100% sub-bituminous coal (100% COAL) sample, the total mass loss reached 95.427%, with the thermal degradation process occurring in two main stages. The first stage occurred within the temperature range of 27.81°C–128.78°C, with a mass loss of 8.007%, which was associated with moisture evaporation and the release of water content. The mass loss during this stage was relatively small. The second stage exhibited the largest mass loss of 80.30%, occurring between 240.21°C and 968.21°C, representing the main combustion phase of fixed carbon. The DTG curve displayed a sharp peak at approximately 370–420°C, indicating a high degradation rate. Above 500°C, the TGA curve gradually became nearly horizontal, indicating that the degradation process had been completed, leaving only char as the combustion residue.

For the 80% coal/20% EFB blend, the TGA and DTG curves exhibited significant changes in the thermal degradation behavior compared with pure coal. The total mass loss increased to 99.08%, indicating that the blended fuel was thermally more degradable. The first degradation stage occurred between 27.3°C and 148.3°C, with a mass loss of 13.767%, corresponding to the release of moisture and other volatile components. The second stage occurred between 185.5°C and 966.3°C, with a mass loss of 82.23%, representing the decomposition of hemicellulose and cellulose contained in the EFB biomass, together with part of the fixed carbon from the coal. The DTG curve exhibited two broader and flatter peaks compared with pure coal, indicating that biomass degradation occurred more gradually. This behavior is attributed to the lignocellulosic structure of biomass, which consists of hemicellulose, cellulose, and lignin that decompose sequentially. Pyrolysis studies of these components have shown that hemicellulose and cellulose decompose within relatively narrow temperature ranges of approximately 220–315°C and 315–400°C, respectively, whereas lignin decomposes slowly over a much wider range of approximately 160–900°C [33], so that the decomposition of lignocellulosic biomass proceeds through overlapping

reactions of its components [34]. This phenomenon is reflected in the TGA curve, which gradually levels off, indicating that most combustible components have decomposed, leaving only ash residue.

For the 60% coal/40% EFB blend, the total mass loss reached 92.196%. The TGA curve showed that the first degradation stage occurred between 27.63°C and 144.1°C, with a mass loss of 9.12%, which was associated with moisture evaporation and water release. The second stage occurred within the temperature range of 185.2°C–965.75°C, resulting in a mass loss of 81.45%, which was attributed to the degradation of volatile compounds and the combustion of fixed carbon, leaving combustion residue. The DTG curve exhibited two broader and more dispersed thermal degradation peaks, indicating that increasing the biomass proportion in the blend shifted the degradation temperature, broadened the thermal degradation range, and produced wider DTG peaks. These characteristics reflect the dominant thermal behavior of biomass, in which thermal reactivity increases but is accompanied by lower thermal stability, as indicated by the shift of the decomposition peaks toward lower temperatures compared with pure coal. Although increasing the EFB content to 40% enhanced the contribution of biomass during combustion and accelerated decomposition, the 20% EFB blend demonstrated superior overall thermal performance in terms of total weight loss, degradation rate, temperature stability, and final residue characteristics, making it more suitable for biomass–coal co-firing applications.

Overall, the TGA and DTG analyses indicate that the addition of Empty Fruit Bunch (EFB) biomass to sub-bituminous coal shifts the degradation temperature, broadens the thermal degradation range, and produces more dispersed DTG peaks. These observations agree with previous TGA studies in which the co-combustion of coal and biomass proceeded through a volatile combustion zone followed by a fixed-carbon combustion zone [23], and in which the addition of biomass enhanced the maximum mass-loss rate and lowered the ignition and burnout temperatures of the blends [17], [20]. These results demonstrate that the incorporation of biomass significantly influences the combustion characteristics and thermal decomposition behavior of coal during the co-firing process.

3.3. Decomposition Kinetic Model

The Coats–Redfern kinetic model is one of the most widely used thermogravimetric analysis methods for evaluating the reaction mechanisms involved in combustion and thermal decomposition of solid materials. This method models the relationship between the reaction conversion degree and temperature using an integral approach, enabling the determination of important kinetic parameters, such as the activation energy (E_a) and the pre-exponential (frequency) factor (A). In the co-firing of sub-bituminous coal with Empty Fruit Bunch (EFB) biomass, the Coats–Redfern model is particularly suitable because it can identify the dominant reaction mechanism at each stage of combustion, including reaction-order, diffusion-controlled, and nucleation-controlled mechanisms [32]. Nevertheless, each kinetic model is interrelated with the others, and although one mechanism may be identified as dominant under certain conditions, this does not imply that the remaining mechanisms are insignificant, as they may also contribute to the overall thermal decomposition process. The conceptual sequence of these model groups is illustrated in **Figure 2**, in which the reaction-order models (F1–F3) are associated with the release of moisture and light volatiles, the diffusion models (D1–D4) with the diffusion of volatile gases, and the Avrami–Erofeev and geometrical contraction models (A2–A3 and R2–R3) with the formation and growth of reaction nuclei and the shrinkage of particles until only the residue remains.

Based on **Table 2**, the results for 100% Coal indicate that, during Stage I, almost all kinetic models produced a coefficient of determination (R^2) greater than 0.90, except for the D1 model. Among the evaluated models, the D3 (Diffusion) model exhibited the highest coefficient of determination, with an R^2 value of 0.93854, indicating excellent agreement between the linear model and the experimental data. This model also produced a slope of −20381.5, reflecting a relatively high activation energy, since a larger slope magnitude corresponds to a higher E_a, which was subsequently used to calculate the activation energy using the Coats–Redfern method. The high R^2 value suggests that the initial thermal degradation of 100% Coal was predominantly governed by an internal diffusion mechanism, indicating that heat-induced chemical reactions occurred mainly within the particle rather than only atits surface. During Stage II, most kinetic models also exhibited R^2 values above 0.90, except for the F2 and F3 models. The D1 (Diffusion) model provided the best fit, with an R^2 of 0.98257 and a slope of − 2703.24, indicating that diffusion-controlled degradation remained the dominant mechanism during the later stage and providing the basis for activation energy calculation using the Coats–Redfern method.

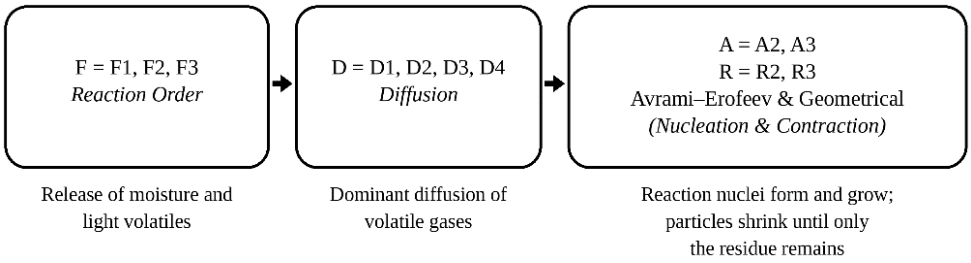


Figure 2. Coats–Redfern kinetic model sequence

Based on the analysis of Table 2, the 20% EFB blend exhibited R^2 values greater than 0.90 for most kinetic models during Stage I. The models with the highest coefficients of determination included F2, F3, D1, D2, D3, A3, R2, and R3. Among these, the R3 (Geometrical Contraction) model provided the best fit, with an R^2 value of 0.93. This high coefficient of determination indicates that the R3 model accurately represents the thermal decomposition mechanism during the initial stage. The corresponding slope of − 7042.429 was subsequently used to determine the activation energy (E_a) using the Coats–Redfern method. The R3 model indicates that the reaction rate is controlled primarily by the physical shrinkage of solid particles. These results suggest that, during the initial stage of thermal degradation, the 20% EFB blend was mainly influenced by moisture evaporation, the release of light volatile compounds, partial combustion of hemicellulose and lignocellulosic components in the EFB, and structural shrinkage of both biomass and coal caused by heating.

Table 2. Kinetic parameters of the eleven Coats–Redfern decomposition models for each fuel sample. Bold values indicate the model with the highest R^2; |Slope| is the absolute value of the regression slope (slope = $-E_a/R$); Average is the arithmetic mean over the eleven models.

Model	Code	Stage I					Stage II				
		|Slope|	Intercept	E_a (kJ/mol)	A (min^{-1})	R^2	|Slope|	Intercept	E_a (kJ/mol)	A (min^{-1})	R^2
COAL 100%											
Reaction order	F1	8948.297	12.16	74.40	1.71×10^{10}	0.92	5362.632	− 5.35	44.58	253.5	0.95
	F2	8709.664	11.41	72.41	7.83×10^{9}	0.92	12070.55	5.30	100.35	2.42×10^{7}	0.86
	F3	9463.653	14.51	78.68	1.90×10^{11}	0.93	23328.49	23.73	193.95	4.72×10^{15}	0.87
Diffusion	D1	7362.882	7.81	61.21	1.82×10^{8}	0.89	**2703.24**	**9.11**	**22.47**	$\mathbf{2.45 \times 10^{8}}$	**0.98**
	D2	18848.63	38.15	156.71	6.96×10^{21}	0.93	7669.242	− 3.65	63.76	2.00×10^{3}	0.98
	D3	**20381.5**	**41.56**	**169.45**	$\mathbf{2.28 \times 10^{23}}$	**0.94**	9709.312	− 1.81	80.72	1.58×10^{4}	0.97
	D4	17070.53	25.23	141.92	1.55×10^{16}	0.92	7445.215	− 11.92	61.90	0.494	0.97
Avrami–Erofeev	A2	4063.728	− 0.98	33.79	1.53×10^{4}	0.91	1961.671	− 10.27	16.31	0.681	0.90
	A3	8061.894	8.24	67.03	3.06×10^{8}	0.91	4533.908	− 7.78	37.69	19.01	0.93
Geometrical contraction	R2	9345.888	12.73	77.70	3.16×10^{10}	0.93	3705.41	− 8.80	30.81	5.56	0.97
	R3	8355.093	9.17	69.46	8.01×10^{8}	0.91	3387.553	− 9.68	28.16	2.12	0.96
Average				**91.16**	$\mathbf{2.13 \times 10^{22}}$				**61.88**	$\mathbf{4.29 \times 10^{14}}$	
EFB 20%:COAL 80%											
Reaction order	F1	7824.273	8.93	65.05	5.89×10^{8}	0.89	3871.994	− 7.39	32.19	23.91	0.94
	F2	8211.485	10.17	68.27	2.14×10^{9}	0.90	16025.68	10.35	133.24	5.03×10^{9}	0.90
	F3	9017.158	13.44	74.97	6.20×10^{10}	0.92	16839.15	14.48	140.00	3.26×10^{11}	0.85
Diffusion	D1	8269.947	11.02	68.76	5.07×10^{9}	0.90	1417.922	− 10.89	11.79	0.265	0.98
	D2	18398.92	37.41	152.97	3.24×10^{21}	0.92	4953.922	− 7.41	41.19	29.90	0.98
	D3	19266.87	38.69	160.18	1.22×10^{22}	0.92	7231.406	− 5.21	60.12	395.7	0.98
	D4	15829.77	21.97	131.61	5.50×10^{14}	0.90	4882.903	− 15.39	40.60	1.01×10^{-2}	0.98
Avrami–Erofeev	A2	3320.607	− 3.17	27.61	1.40×10^{3}	0.86	1560.708	− 10.82	12.98	0.311	0.92
	A3	8767.488	10.83	72.89	4.43×10^{9}	0.91	3451.038	− 9.12	28.69	3.79	0.93
Geometrical contraction	R2	8754.199	11.19	72.78	6.33×10^{9}	0.91	2284.643	− 10.75	18.99	0.489	0.97
	R3	**7042.429**	**5.53**	**58.55**	$\mathbf{1.78 \times 10^{7}}$	**0.93**	**1913.352**	**− 11.72**	**15.91**	**0.155**	**0.98**
Average				**86.69**	$\mathbf{1.41 \times 10^{21}}$				**48.70**	$\mathbf{3.01 \times 10^{10}}$	
EFB 40%:COAL 60%											
Reaction order	F1	9005.886	12.52	74.87	2.47×10^{10}	0.91	4367.826	− 6.39	36.31	73.32	0.96
	F2	9748.274	14.91	81.05	2.90×10^{11}	0.93	10991.9	4.72	91.39	1.23×10^{7}	0.81
	F3	**10339.89**	**17.51**	**85.97**	$\mathbf{4.15 \times 10^{12}}$	**0.93**	18502.06	18.23	153.83	1.53×10^{13}	0.80
Diffusion	D1	8257.416	10.82	68.65	4.12×10^{9}	0.90	1984.083	− 9.91	16.50	0.981	0.97
	D2	17645.44	34.66	146.70	2.00×10^{20}	0.91	**6019.593**	**− 5.50**	**50.05**	**246.7**	**0.99**
	D3	17281.33	32.00	143.68	1.37×10^{19}	0.91	6919.711	− 5.26	57.53	359.5	0.98
	D4	19177.91	32.32	159.45	2.08×10^{19}	0.92	5837.107	− 13.65	48.53	6.86×10^{-2}	0.99
Avrami–Erofeev	A2	3878.939	− 1.48	32.25	8.84×10^{3}	0.89	1293.854	− 11.07	10.76	0.201	0.92
	A3	8401.638	9.49	69.85	1.12×10^{9}	0.90	3808.598	− 8.38	31.66	8.69	0.96
Geometrical contraction	R2	9195.371	12.43	76.45	2.30×10^{10}	0.92	2730.843	− 9.92	22.70	1.34	0.99
	R3	8318.634	9.23	69.16	8.46×10^{8}	0.90	3040.755	− 9.76	25.28	1.75	0.98
Average				**91.64**	$\mathbf{2.13 \times 10^{19}}$				**49.50**	$\mathbf{1.39 \times 10^{12}}$	

During Stage II, Table 2 shows that almost all kinetic models produced R^2 values greater than 0.90, except for the F3 model. The R3 model again provided the best agreement with the experimental data, with an R^2 value of 0.98496 and a slope of −1913.352, which was used to calculate the activation energy using the Coats–Redfern method. At this stage, the R3 model indicates that combustion was predominantly controlled by the three-dimensional contraction of the reacting core. In other words, the reaction rate was governed not only by surface chemical reactions but also by the continuous reduction in the size and volume of the solid particles. This chemical reactions but also by the continuous reduction in the size and volume of the solid particles. This represents a mechanism in which the solid matrix gradually contracts as gaseous products diffuse outward, eventually leading to complete consumption of the solid particles as the reaction proceeds throughout the entire particle volume.

For the 40% EFB/60% Coal blend, Table 2 shows that almost all kinetic models yielded R^2 values of at least 0.90 during Stage I, except the A2 model (0.89), with the highest value obtained for the F3 (Third-Order Reaction) model, which produced an R^2 value of 0.93313. This high coefficient of determination suggests that the thermal decomposition mechanism at the initial stage was relatively complex, involving a reaction behavior that was best represented by a third-order reaction model. This phenomenon may be associated with the release of volatile compounds from hemicellulose and part of the cellulose contained in the EFB during the early heating stage, thereby accelerating the chemical reaction rate and making the third-order kinetic model more appropriate for describing the degradation process.

During Stage II, the highest coefficient of determination was obtained for the D2 (Diffusion) model, with an R^2 value of 0.99174 and a slope of −6019.593, which was subsequently used to calculate the activation energy (E_a). The D2 model represents a mechanism in which the reaction rate is controlled by the two-dimensional diffusion of reactant molecules across the particle surface. In the combustion of the 40% EFB/60% COAL blend, this indicates that after the major volatile components had been released during the initial stage, the subsequent reaction became increasingly controlled by diffusion resistance resulting from the formation of carbonaceous or ash layers on the particle surface. These layers hindered the release of the remaining gaseous products, causing the overall reaction rate to become diffusion-controlled.

These findings are consistent with the theory of solid-state reactions described by Ropp [32], who reported that the reaction rate of solid materials may be governed by several principal mechanisms, including reaction-order models (F1–F3), diffusion models (D1–D4), nucleation models (A1–A3), geometrical contraction models (R1–R3), and phase boundary-controlled models. The dominant mechanism depends on the stage of thermal decomposition, the characteristics of the material, and the structural changes induced by heating. The dominance of diffusion models in the char combustion stage of pure coal and the 40% EFB blend is in line with Guo *et al.* [21], who found that the D3 and D4 diffusion models best described the second stage of biomass combustion and the combustion of lignite, respectively, in coal–biomass pellet blends. Likewise, the change in the best-fitting model between combustion stages agrees with the finding that different subdivisions of EFB decomposition are described by different reaction models [29].

3.4. Activation Energy

Activation energy is one of the principal parameters in reaction kinetics because it represents the minimum amount of energy required to initiate the thermal decomposition process of a material. The activation energy is commonly determined from thermogravimetric analysis (TGA) using an appropriate mathematical model. One of the most widely applied approaches is the Coats–Redfern method, which is used to determine kinetic parameters based on thermogravimetric analysis (TGA) data. The calculation of the activation energy (E_a) and the coefficient of determination (R^2) was performed to evaluate the thermal degradation mechanism of the fuels. This calculation is based on a non-isothermal kinetic model using the integral function g(α), which represents the reaction mechanism of solid materials during the thermal decomposition process. The activation energy was determined from the plot of $\ln(g(\alpha)/T^2)$ versus $1/T$. A linear relationship indicates that the selected kinetic model is consistent with the experimental data. The activation energy was calculated from the slope of the linear regression, while the pre-exponential factor was determined from the intercept of the regression line [25], [26]. The calculations and regression analysis were performed using Origin software.

Based on the activation energy (E_a) values presented in Figure 3, the reported values represent the average activation energy obtained from all kinetic models evaluated for each reaction stage using the Coats–Redfern

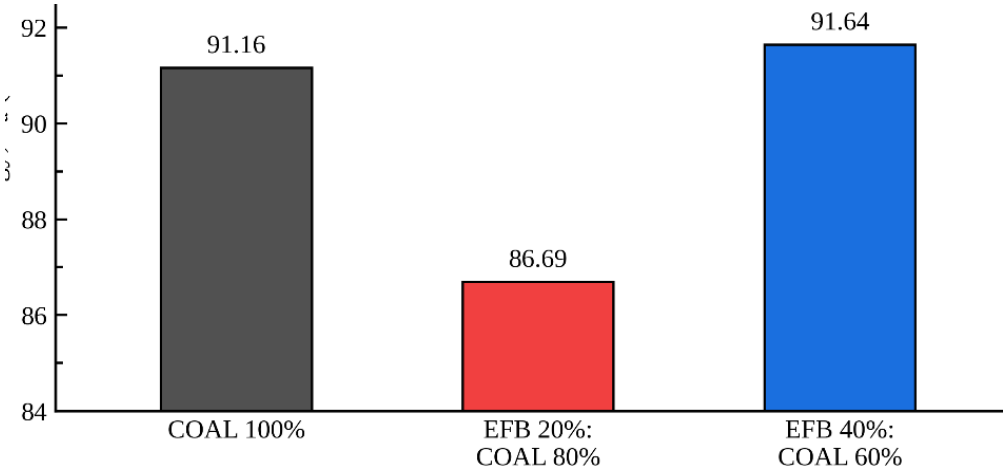


Figure 3.
Average activation energy (E_a) of the fuel samples in Stage I

method. Averaging the activation energy across different kinetic models was intended to reduce the bias associated with selecting a single dominant model when several models exhibited similarly good agreement with the experimental data. During the initial stage, which generally corresponds to the devolatilization process, the addition of 20% EFB reduced the average activation energy from 91.16 kJ/mol for 100% COAL to 86.69 kJ/mol, indicating enhanced initial reactivity. This reduction can be attributed to the high contents of cellulose, hemicellulose, and volatile matter in the EFB, which decompose more readily at relatively low temperatures and promote the formation of initial pore structures that facilitate the release of volatile gases. A reduction in the apparent activation energy upon blending oil palm biomass with sub-bituminous coal was also reported by Idris *et al.* [17]. However, when the EFB proportion was increased to 40%, the average activation energy increased to 91.64 kJ/mol. This increase may reflect a change in the dominant reaction mechanism, such as a shift toward diffusion-controlled or geometrical contraction mechanisms, or the influence of biomass ash composition, which alters the reaction pathway within specific conversion ranges. This non-monotonic trend differs from the continuous decrease in activation energy with increasing biomass fraction reported by Yuan *et al.* [20] for agricultural residues, but it is consistent with Guo *et al.* [21], who obtained the minimum activation energy at an intermediate biomass ratio rather than at the highest one.

During Stage II, as shown in the activation energy (E_a) chart in **Figure 4**, pure coal exhibited a relatively high activation energy of 61.88 kJ/mol, indicating that the combustion of the residual coal char requires a relatively large amount of energy because of its low porosity and the absence of catalytic mineral species. With the addition of 20% EFB, the average activation energy decreased markedly to 48.70 kJ/mol, which is consistent with the increased porosity of the resulting char and the presence of alkali and alkaline earth metals, particularly potassium and calcium, in the EFB ash [7]. These minerals can act as catalysts that accelerate carbon oxidation during char combustion, and the catalytic contribution of biomass-derived minerals to the synergistic effects observed during the co-processing of coal and biomass has been demonstrated experimentally [22]. However, when the EFB content was increased to 40%, the average activation energy increased slightly to 49.50 kJ/mol, although it remained lower

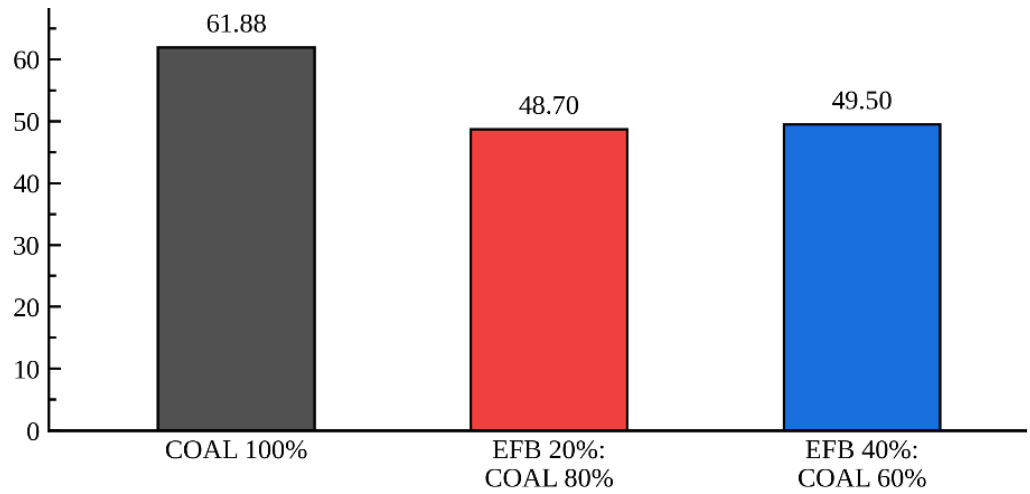


Figure 4.
Average activation energy (E_a) of the fuel samples in Stage II

than that of pure coal. Overall, these results indicate that the addition of 20% EFB produces a positive synergistic effect, as evidenced by the reduction in activation energy during both the devolatilization and char oxidation stages. At a higher blending ratio (40% EFB), however, this synergistic effect diminished, likely due to the increased contribution of lignin and the formation of an ash layer on the char surface, which inhibited the combustion process. A higher EFB fraction also increases the input of alkali- and silica-bearing ash, which is associated with a greater slagging and fouling tendency during co-firing [9], [10]; therefore, the 20% EFB blend offers a better compromise between kinetic reactivity and ash-related risks. Finally, because the kinetic parameters in this study were obtained by model fitting at a single heating rate, they should be regarded as apparent values, and verification using multiple heating rates and isoconversional methods is recommended [31].

4. Conclusion

This study investigated the effect of blending ratios on the co-firing process of sub-bituminous coal and Empty Fruit Bunch (EFB) biomass. Thermogravimetric analysis showed that the combustion of pure sub-bituminous coal and its blends with EFB occurred in two main stages: the release of moisture and light volatile compounds, followed by the combustion of fixed carbon. For pure coal, the greatest mass degradation occurred within the temperature range of 240.21–968.21°C, with a mass loss of approximately 80.30%. The addition of 20% EFB increased the total mass loss to 99.08%, accompanied by a higher initial volatile release of 13.77%, indicating that the biomass accelerated the devolatilization process. In contrast, the 40% EFB blend exhibited a total mass loss of 92.20% with a broader DTG peak, suggesting higher reactivity but lower thermal stability than pure coal. Overall, the addition of EFB broadened the degradation temperature range, enhanced volatile release, and accelerated the thermal decomposition of the blended fuel.

Kinetic analysis using the Coats–Redfern approach demonstrated that each fuel sample exhibited a different dominant kinetic model at each combustion stage. Increasing the proportion of EFB in the blend altered the dominant decomposition mechanism, shifting from diffusion-controlled mechanisms in pure coal toward geometrical contraction and higher-order reaction mechanisms due to the influence of the biomass. Nevertheless, although one kinetic model may provide the best fit under specific conditions, this does not imply that the remaining kinetic models are insignificant, as multiple reaction mechanisms may simultaneously contribute to the overall thermal decomposition process.

The activation energy (E_a) also varied among the different fuel blends. In Stage I, pure coal exhibited an average activation energy of 91.16 kJ/mol, indicating relatively high thermal stability but lower reactivity. The addition of 20% EFB reduced the average activation energy to 86.69 kJ/mol, suggesting that thermal decomposition occurred more readily, whereas increasing the EFB content to 40% raised the average activation energy to 91.64 kJ/mol. These results indicate that the addition of EFB significantly influences the activation energy of the co-firing process. Among the tested blends, the 20% EFB mixture exhibited the highest reactivity, whereas the 40% EFB blend required greater energy for decomposition because of the more complex thermal degradation behavior of the biomass. A similar trend was observed in Stage II (char combustion), where the average activation energy decreased from 61.88 kJ/mol for pure coal to 48.70 kJ/mol for the 20% EFB blend and increased slightly to 49.50 kJ/mol for the 40% EFB blend, although it remained lower than that of pure coal. Therefore, the 20% EFB blend represents the optimum co-firing ratio from a kinetic perspective.

Acknowledgements - The authors would like to thank the reviewers for their valuable comments and suggestions, which helped sharpen this article.

Conflict of Interest - The authors declare that there are no conflicts of interest.

CRediT Author Statement - **AFA**: Methodology, Validation, Visualization, Writing – Review & Editing; **NM**: Investigation, Data Curation, Formal Analysis, Writing – Original Draft; **EM**: Conceptualization, Supervision, Writing – Review & Editing.**RA**: Supervision, Writing – Review & Editing.

Funding – This research received no specific grant from any funding agency in the public, commercial, or not-for-profit sectors.

Gen AI Statement - The authors used Claude to improve the grammar of the manuscript. All AI-assisted revisions were reviewed and verified by the authors, who take full responsibility for the content of the final manuscript.

References

[1] A. Sugiyono *et al.*, "Strategies toward energy transition in Indonesia: An assessment of multi-regional biomass supply for coal co-firing power plants," *International Journal of Sustainable Energy Planning and Management*, vol. 47, pp. 43–56, 2025, doi: 10.54337/ijsepm.10514.

[2] M. S. Roni, S. Chowdhury, S. Mamun, M. Marufuzzaman, W. Lein, and S. Johnson, "Biomass co-firing technology with policies, challenges, and opportunities: A global review," *Renewable and Sustainable Energy Reviews*, vol. 78, pp. 1089–1101, 2017, doi: 10.1016/j.rser.2017.05.023.

[3] Z. Arifin, V. F. S. Insani, M. Idris, K. R. Hadiyati, Z. Anugia, and D. Irianto, "Techno-economic analysis of co-firing for pulverized coal boilers power plant in Indonesia," *International Journal of Renewable Energy Development*, vol. 12, no. 2, pp. 261–269, 2023, doi: 10.14710/ijred.2023.48102.

[4] M. A. Rahmanta, A. Aprilana, Ruly, N. Cahyo, T. W. D. Hapsari, and E. Supriyanto, "Techno-economic and environmental impact of biomass co-firing with carbon capture and storage in Indonesian power plants," *Sustainability*, vol. 16, no. 8, p. 3423, 2024, doi: 10.3390/su16083423.

[5] E. I. Rhofita, R. Rachmat, M. Meyer, and L. Montastruc, "Mapping analysis of biomass residue valorization as the future green energy generation in Indonesia," *Journal of Cleaner Production*, vol. 354, p. 131667, 2022, doi: 10.1016/j.jclepro.2022.131667.

[6] Ministry of Agriculture, *Statistical of National Leading Estate Crops Commodity 2021–2023*. Jakarta, Indonesia: Directorate General of Estate Crops, 2022.

[7] C. Hendrasetiafitri, Y. J. Sung, and D.-S. Kim, "Effects of pretreatments on the chemical composition and thermal conversion of oil palm empty fruit bunch," *BioResources*, vol. 17, no. 2, pp. 2727–2742, 2022, doi: 10.15376/biores.17.2.2727-2742.

[8] Mahidin *et al.*, "Analysis of power from palm oil solid waste for biomass power plants: A case study in Aceh Province," *Chemosphere*, vol. 253, p. 126714, 2020, doi: 10.1016/j.chemosphere.2020.126714.

[9] Y. Niu, H. Tan, and S. Hui, "Ash-related issues during biomass combustion: Alkali-induced slagging, silicate melt-induced slagging (ash fusion), agglomeration, corrosion, ash utilization, and related countermeasures," *Progress in Energy and Combustion Science*, vol. 52, pp. 1–61, 2016, doi: 10.1016/j.pecs.2015.09.003.

[10] Hariana, Prabowo, E. Hilmawan, F. M. Kuswa, A. Darmawan, and M. Aziz, "A comprehensive evaluation of cofiring biomass with coal and slagging-fouling tendency in pulverized coal-fired boilers," *Ain Shams Engineering Journal*, vol. 14, no. 7, p. 102001, 2023, doi: 10.1016/j.asej.2022.102001.

[11] Hariana *et al.*, "Theoretical and experimental investigation of ash-related problems during coal co-firing with different types of biomass in a pulverized coal-fired boiler," *Energy*, vol. 269, p. 126784, 2023, doi: 10.1016/j.energy.2023.126784.

[12] I. B. Novendianto *et al.*, "Investigation of the slagging and fouling aspects of co-firing coal and organic refuse-derived fuel," *Thermal Science and Engineering Progress*, vol. 49, p. 102447, 2024, doi: 10.1016/j.tsep.2024.102447.

[13] B. Yousaf *et al.*, "Systematic investigation on combustion characteristics and emission-reduction mechanism of potentially toxic elements in biomass- and biochar-coal co-combustion systems," *Applied Energy*, vol. 208, pp. 142–157, 2017, doi: 10.1016/j.apenergy.2017.10.059.

[14] M. Soh, J. J. Chew, S. Liu, and J. Sunarso, "Comprehensive kinetic study on the pyrolysis and combustion behaviours of five oil palm biomass by thermogravimetric–mass spectrometry (TG–MS) analyses," *BioEnergy Research*, vol. 12, no. 2, pp. 370–387, 2019, doi: 10.1007/s12155-019-09974-9.

[15] Y. J. Rueda-Ordóñez, C. J. Arias-Hernández, J. F. Manrique-Pinto, P. Gauthier-Maradei, and W. A. Bizzo, "Assessment of the thermal decomposition kinetics of empty fruit bunch, kernel shell and their blend," *Bioresource Technology*, vol. 292, p. 121923, 2019, doi: 10.1016/j.biortech.2019.121923.

[16] B. Castells, I. Amez, L. Medic, and J. García-Torrent, "Torrefaction influence on combustion kinetics of Malaysian oil palm wastes," *Fuel Processing Technology*, vol. 218, p. 106843, 2021, doi: 10.1016/j.fuproc.2021.106843.

[17] S. S. Idris, N. A. Rahman, and K. Ismail, "Combustion characteristics of Malaysian oil palm biomass, sub-bituminous coal and their respective blends via thermogravimetric analysis (TGA)," *Bioresource Technology*, vol. 123, pp. 581–591, 2012, doi: 10.1016/j.biortech.2012.07.065.

[18] N. S. Hamzah, S. S. Idris, N. A. Rahman, N. F. Abu Bakar, and S. Matali, "Thermal analysis of co-utilization of empty fruit bunch and Silantek coal under inert atmosphere using thermogravimetric analyzer (TGA)," *Frontiers in Energy Research*, vol. 8, p. 608756, 2021, doi: 10.3389/fenrg.2020.608756.

[19] M. Z. E. Prayoga *et al.*, "Co-combustion performance of oil palm biomass with coal: Thermodynamics and kinetics analyses," *Journal of Thermal Analysis and Calorimetry*, vol. 149, no. 7, pp. 2873–2891, 2024, doi: 10.1007/s10973-023-12865-z.

[20] Y. Yuan, Y. He, J. Tan, Y. Wang, S. Kumar, and Z. Wang, "Co-combustion characteristics of typical biomass

and coal blends by thermogravimetric analysis," *Frontiers in Energy Research*, vol. 9, p. 753622, 2021, doi: 10.3389/fenrg.2021.753622.

[21] F. Guo, Y. He, A. Hassanpour, J. Gardy, and Z. Zhong, "Thermogravimetric analysis on the co-combustion of biomass pellets with lignite and bituminous coal," *Energy*, vol. 197, p. 117147, 2020, doi: 10.1016/j.energy.2020.117147.

[22] J. M. Oladejo, S. Adegbite, C. H. Pang, H. Liu, A. M. Parvez, and T. Wu, "A novel index for the study of synergistic effects during the co-processing of coal and biomass," *Applied Energy*, vol. 188, pp. 215–225, 2017, doi: 10.1016/j.apenergy.2016.12.005.

[23] S. Sezer, F. Kartal, and U. Özveren, "The investigation of co-combustion process for synergistic effects using thermogravimetric and kinetic analysis with combustion index," *Thermal Science and Engineering Progress*, vol. 23, p. 100889, 2021, doi: 10.1016/j.tsep.2021.100889.

[24] Z. Xiao, S. Wang, M. Luo, and J. Cai, "Combustion characteristics and synergistic effects during co-combustion of lignite and lignocellulosic components under oxy-fuel condition," *Fuel*, vol. 310, p. 122399, 2022, doi: 10.1016/j.fuel.2021.122399.

[25] M. Raza, B. Abu-Jdayil, A. H. Al-Marzouqi, and A. Inayat, "Kinetic and thermodynamic analyses of date palm surface fibers pyrolysis using Coats-Redfern method," *Renewable Energy*, vol. 183, pp. 67–77, 2022, doi: 10.1016/j.renene.2021.10.065.

[26] S. R. Naqvi *et al.*, "Pyrolysis of high ash sewage sludge: Kinetics and thermodynamic analysis using Coats-Redfern method," *Renewable Energy*, vol. 131, pp. 854–860, 2019, doi: 10.1016/j.renene.2018.07.094.

[27] H. Gohar *et al.*, "Investigating the characterisation, kinetic mechanism, and thermodynamic behaviour of coal-biomass blends in co-pyrolysis process," *Process Safety and Environmental Protection*, vol. 163, pp. 645–658, 2022, doi: 10.1016/j.psep.2022.05.063.

[28] F. Surahmanto, H. Saptoadi, H. Sulistyo, and T. A. Rohmat, "Investigation of the pyrolysis characteristics and kinetics of oil-palm solid waste by using Coats–Redfern method," *Energy Exploration & Exploitation*, vol. 38, no. 1, pp. 298–309, 2020, doi: 10.1177/0144598719877759.

[29] A. H. Supee and M. A. A. Zaini, "Kinetics, thermodynamics, and thermal decomposition behavior of palm oil empty fruit bunch, coconut shell, bamboo, and cardboard pyrolysis: An integrated approach using Coats–Redfern method," *Environmental Monitoring and Assessment*, vol. 195, no. 10, p. 1218, 2023, doi: 10.1007/s10661-023-11866-7.

[30] F. J. F. Phang *et al.*, "Hydrochars derived via wet torrefaction of empty fruit bunches: Effect of temperature and time, comparison to oil palm trunks counterpart, and their pyrolysis behavior," *Journal of Analytical and Applied Pyrolysis*, vol. 179, p. 106441, 2024, doi: 10.1016/j.jaap.2024.106441.

[31] N. Koga *et al.*, "ICTAC Kinetics Committee recommendations for analysis of thermal decomposition kinetics," *Thermochimica Acta*, vol. 719, p. 179384, 2023, doi: 10.1016/j.tca.2022.179384.

[32] R. C. Ropp, "Mechanisms and reactions in the solid state," in *Solid State Chemistry*, Amsterdam, The Netherlands: Elsevier, 2003. doi: 10.1016/B978-044451436-3/50004-3.

[33] H. Yang, R. Yan, H. Chen, D. H. Lee, and C. Zheng, "Characteristics of hemicellulose, cellulose and lignin pyrolysis," *Fuel*, vol. 86, no. 12–13, pp. 1781–1788, 2007, doi: 10.1016/j.fuel.2006.12.013.

[34] R. Xiao *et al.*, "Thermogravimetric analysis and reaction kinetics of lignocellulosic biomass pyrolysis," *Energy*, vol. 201, p. 117537, 2020, doi: 10.1016/j.energy.2020.117537.